

Crack monitoring around a hole under mixed mode (I+II) loading by image correlation

P. López-Crespo¹, A. Shterenlikht², J. R. Yates¹, E. A. Patterson³, P. J. Withers² and R. Burguete⁴

¹ Mechanical Engineering Department, Sheffield University, Mappin Street, Sheffield S1 3JD, UK

² Materials Science Centre, Manchester University, Grosvenor Street, Manchester M1 7HS, UK

³ Mechanical Engineering, Michigan State University, 2555 Engineering Building, East Lansing, MI 48824-1226, USA

⁴ Airbus UK, New Filton House, Filton, Bristol, BS99 7AR, UK

ABSTRACT. *Fastening holes are critical in the aircraft industry from a structural integrity viewpoint. This is because they act as stress concentrators from which cracks often grow. In this work the image correlation technique has been used to measure displacements near a crack tip under mixed mode (I+II) stress field on Al 7010 samples. The crack tip position was deduced from the shape of the displacement fields. Then analytical displacement fields have been fitted to the experimental data by combining Muskhelishvili's complex function approach with conformal mapping and multiple point over-deterministic method to infer SIFs. The mode I experimentally calculated SIFs overall agree well with the theoretical applied values, with the maximum difference less than 10%. The agreement for the mode II SIF was not as good as for mode I, although the differences between calculated and nominal values are comparable to those obtained for mode I. Probably the signal to noise ratio is the main reason for this discrepancy, as in all the cases nominal K_I were several times bigger than K_{II} .*

INTRODUCTION

Many components, especially in aircraft structures, need holes to allow for fastenings. These holes are stress concentrators from which cracks often grow, making them critical areas from a structural integrity viewpoint. The service life of the components can be estimated through the stress intensity factor (SIF).

Different full-field experimental techniques have been employed for SIF calculation [1-3]. However all have very specific requirements which make them suitable only for laboratory studies. Photoelasticity needs either a plastic model or the bonding of a coating to the specimen. Moiré interferometry requires a grating to be applied to the specimen, while thermoelasticity requires that the load be applied cyclically. Recently image correlation has matured into a stable and reliable measuring tool. By contrast it is

very cheap, fast and much easier to apply experimentally than the above methods. In addition the IC technique requires minimal or no surface preparation but measures displacement rather than properties linked directly to strain or stress.

Previously, some work has been done on SIF calculation by image correlation techniques [4, 5]. However these approaches have been limited by the application of a simplified crack tip stress field, e.g. Westergaard solution, where the influence of the boundary conditions is ignored. Moreover, the authors also used artificially generated cracks in compliant materials instead of sharp fatigue cracks, in uniform passing stress fields.

In this work we have applied a very powerful Muskhelishvili's complex function analysis to determine stress intensity factors from displacement fields around a sharp fatigue crack. The crack was grown from a stress concentrator, thus generating a non-uniform passing stress field.

IMAGE CORRELATION TECHNIQUE

A number of image correlation algorithms have been developed, see e.g. [6; 7], and the number of commercial and research IC packages is steadily growing. Accordingly the need for an IC standard for assessing their capability for engineering applications is recognised [8].

The principle of the IC method is simple [9]. A digital image comprises a two-dimensional array of intensity values, $I(x,y)$. Given two images, I_A and I_B , a $N \times N$ pixel region of interest, patch, is defined in each image. If the image brightness is approximately constant, $\sum I_A^2 \approx \sum I_B^2$, then a measure of the similarity between the two regions of interest can be expressed as a cross-correlation product [6]:

$$c(u,v) = \sum_{x=-n}^n \sum_{y=-n}^n I_A(x,y) I_B(x+u,y+v), \quad (1)$$

where u and v are the distances between the centres of the two regions of interest along x and y accordingly, and $n=N/2$.

If I_A is an image of some object and I_B is another image of the same object after it undergone some deformation or rigid body movement, then the maximum of the cross-correlation function (1) gives the most probable displacement values for the centre of the region of interest in I_A .

In this work a commercial IC package, DaVis by LaVision, was used. In this implementation the images are first transformed into the frequency domain using a fast Fourier transform. Then the cross-correlation function (1) is calculated in the frequency domain. This proves to be several times faster than using (1) in the spatial domain [9].

MUSKHELISHVILI'S COMPLEX FUNCTION ANALYSIS

Since the IC method measures displacement fields, it is advantageous to derive the relationship between displacements and SIF. This can be done using Muskhelishvili's complex function analysis. Let's consider a plane body lying in a complex plane Z . Displacements in Z can be expressed through two analytical functions of complex variable, $\phi = \phi(z)$ and $\psi = \psi(z)$, where $z = x + iy$, as follows [11]:

$$2\mu(u + iv) = \chi\phi(z) - z\phi'(z) - \psi(z) \quad (2)$$

where

$$\mu = \frac{E}{2(1+\nu)}; \quad \chi = 3 - 4\nu \text{ (plane strain); } \chi = \frac{3-\nu}{1+\nu} \text{ (plane stress)} \quad (3)$$

u and v are displacements and σ_{ij} are stresses, $i, j = 1, 2$. E is the Young's modulus and ν is the Poisson's ratio. The overbar denotes the complex conjugate and the prime denotes the first derivative.

The function

$$z = \omega(\zeta) = R \left(\zeta + \frac{m}{\zeta} \right) \quad (4)$$

where m is a shape parameter, $0 \leq m \leq 1$, and R is a scale parameter which maps a unit circle onto an elliptical contour, L , in plane Z . If $m=1$ then L is an idealized crack of zero thickness and length $4R$.

The analytical functions in the mapping plane $\phi(\zeta)$ and $\psi(\zeta)$ can be represented by an infinite Fourier series:

$$\phi(\zeta) = \sum_{k=-\infty}^{+\infty} a_k \zeta^k; \quad \text{and} \quad \psi(\zeta) = \sum_{k=-\infty}^{+\infty} b_k \zeta^k \quad (5)$$

where a_k and b_k are complex coefficients.

It can be shown after a lengthy derivation that (2), (4) and (5) and the satisfaction of the traction-free crack boundary condition lead to the following system of real linear equations written for p experimental sampling points:

$$\sum_{k=-N}^N A_k^j \alpha_k + \sum_{k=-N}^N B_k^j \beta_k = 2\mu u^j \quad (6)$$

$$\sum_{k=-N}^N C_k^j \alpha_k + \sum_{k=-N}^N D_k^j \beta_k = 2\mu v^j \quad (7)$$

where $j=1,2,\dots,p$, u^j and v^j are displacements at point j , A_k^j , B_k^j , C_k^j and D_k^j are coefficients which depend on ζ calculated at point j , and $\alpha_k = \text{Re}(a_k)$ and $\beta_k = \text{Im}(a_k)$.

The system (6)-(7) has $2N+1$ unknowns α_k and $2N+1$ unknowns β_k or $2(2N+1)$ unknowns in total. If $p > 2N+1$ then the number of unknowns is smaller than the number of equations and the system is overdetermined. The solution can be found in the linear least squares sense.

It was shown in [12] that the complex stress intensity factor

$$K = K_I - iK_{II} \quad (8)$$

can be found as

$$K = 2\sqrt{2\pi} \lim_{\zeta \rightarrow 1} \left\{ \phi'(\zeta) \frac{\sqrt{\varpi(\zeta) - \varpi(1)}}{\varpi'(\zeta)} \right\} \quad (9)$$

Note the factor $\sqrt{\pi}$ which does not appear in [12].

Using (4) with $m=1$ and (5) one obtains:

$$K = 2\sqrt{\frac{\pi}{a}} \sum_{k=-N}^N k a_k \quad (10)$$

where $a = 2R$ is a half length of a centre crack in an infinite plane. This value is obtained from (4) by noting that $z = a$ corresponds to $\zeta = 1$.

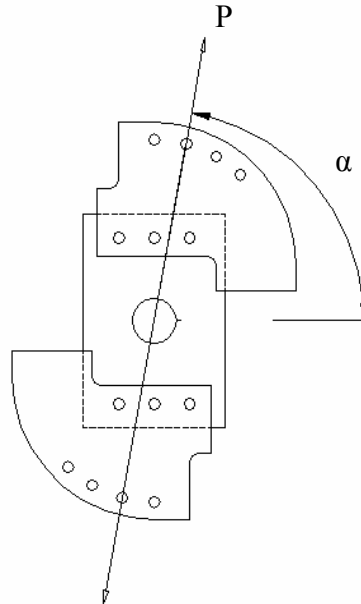


Figure 1: Geometry of the specimen and grips allowing different degrees of mixed mode, α .

EXPERIMENTAL PROCEDURE

The plate used was 160 mm (w) x 240 mm (l) with a 50 mm diameter centred hole. It was made of 5 mm thick aluminium alloy (Al 7010 T7651). To initiate the crack, two 2 mm deep notches were introduced emanating either side of the sample, so that the crack grew perpendicular to the loading axis when pure mode I load is applied to the specimen ($\alpha = 90^\circ$ in Fig. 1). A fine disk saw of 0.15 mm thickness was used for this purpose.

The crack was grown under mode I by applying cyclic loading, with load ratio $K_{\min}/K_{\max} = 0.1$ and stress intensity factor range $\Delta K = 10 \text{ MPa}\sqrt{\text{m}}$. 380,000 cycles were applied at a frequency of 10 Hz. Subsequently the crack length on either side of the sample was measured with an optical microscope to be 5.25 mm and 4.70 mm long.

The mixed mode loading grips with the specimen used are shown in Fig. 1. The specimen was loaded under load control. The maximum applied load was 25 kN.

The sample surface was scratched, with 120 and 400 grit SiC paper giving sufficient contrast for the IC. Two sources of light were positioned around the specimen to obtain uniform intensity. The images were acquired with a 1600×1200 pixel CCD camera. An example of a captured image is shown in Fig. 2. The resolution was $20 \mu\text{m}$ per pixel.

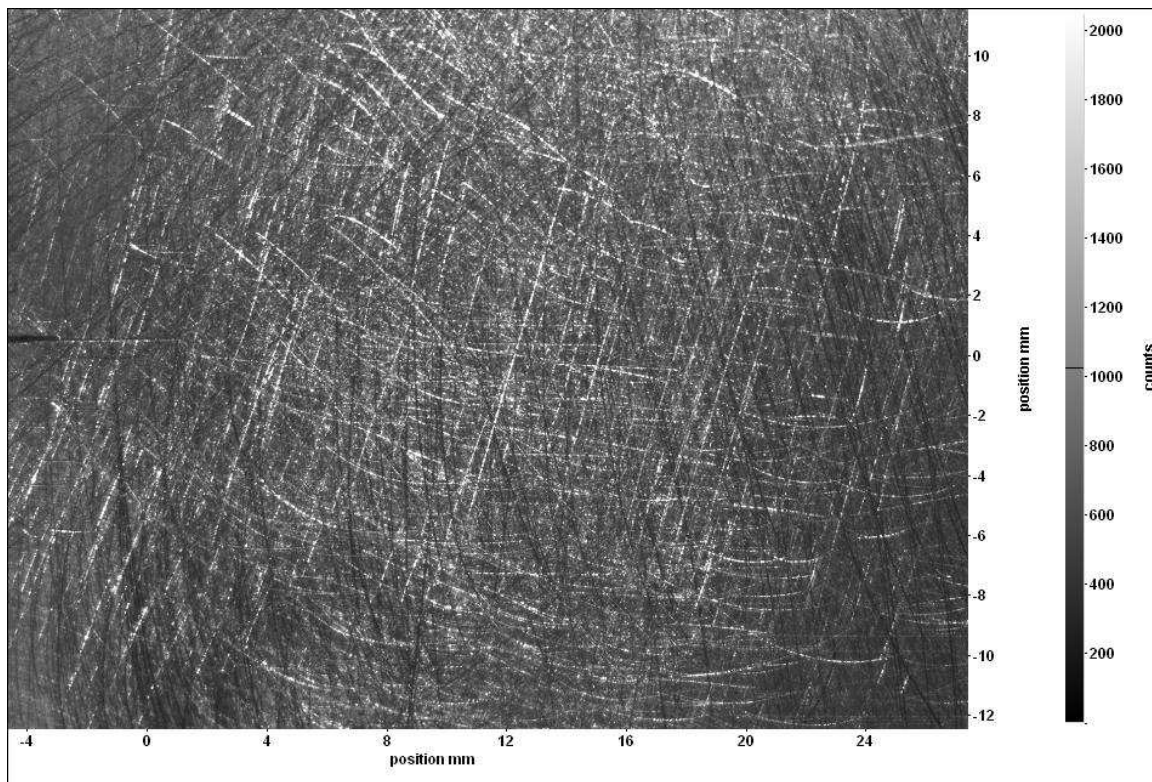


Figure 2: A 1600×1200 pixel image of the specimen surface. The resolution is $20.1 \mu\text{m}$ per pixel. The origin of coordinates is located at the crack tip of the fatigue crack. The image shows the state at maximum load (25 kN).

The image correlation was performed with DaVis 7 program [10] using 32×32 pixel image patches overlapped by 50 %.

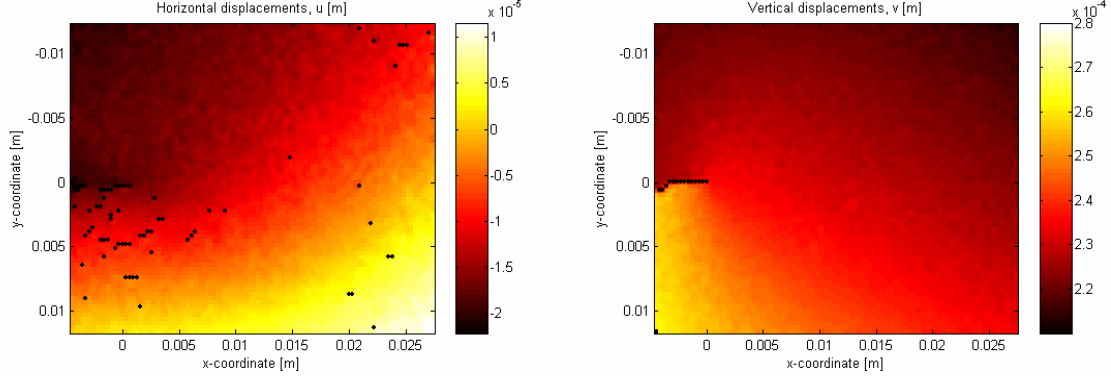


Figure 3: Edges detected with Prewitt edge finding method. The displacement fields shown was obtained for $\alpha = 79.65^\circ$. At this mixity the vertical displacement gives the better result.

RESULTS

Fig. 2 was obtained at maximum applied load. Nevertheless, as is typical for most fatigue cracks, the crack can not be easily discerned by visual inspection. However the influence of the crack tip location is a major issue for experimental SIF calculation [13]. For that reason the crack tip was located automatically by applying an edge finding method [14]. The Prewitt operator was used to detect the crack by identifying sharp changes in the intensity of the displacement fields (see Fig. 3). Once the crack tip was found, it was assigned the coordinates (0,0). The displacement was acquired at approx. 2500 points around the crack (Fig. 4). The data collected was employed to solve by QR decomposition [15] the linear system of equations. The results are shown in Table 1 and also in Fig. 5. The nominal applied SIF were calculated from the solution for an inclined crack emanating from an elliptical hole under tension given in [16].

Table 1: Results for different angles between the load axis and the crack

α , degrees	$K_{I \text{ theo}}$, MPa $\sqrt{\text{m}}$	$K_{I \text{ exp}}$, MPa $\sqrt{\text{m}}$	$K_{II \text{ theo}}$, MPa $\sqrt{\text{m}}$	$K_{II \text{ exp}}$, MPa $\sqrt{\text{m}}$
90	13.52	14.75	0	0.59
79.65	13.81	13.62	1.53	0.79
69.05	13.17	13.33	3.12	1.05
58.45	12.38	10.50	4.30	4.91

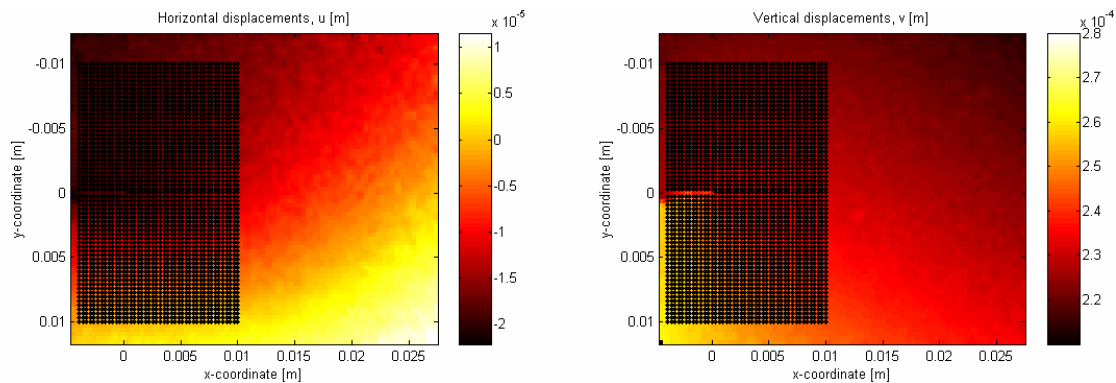


Figure 4: Typical array with selected displacement points considered for the SIF calculation. The displacement fields shown was obtained for $\alpha = 79.65^\circ$.

DISCUSSION

One of the sources of discrepancy between the nominal and measured SIF may be that the fatigue crack was grown under pure mode I conditions, and the same crack was used for all the mixed mode analyses.

The mode I experimentally calculated SIFs overall agree well with the theoretical applied values, with the maximum difference less than 10%. The agreement for the mode II SIF was not as good as for mode I, although the differences between calculated and nominal values are comparable to those obtained for mode I. Probably the signal to noise ratio is the main reason for this discrepancy, as in all the cases nominal K_I were several times bigger than K_{II} .

Other sources of uncertainty may be the deviation from ideal conditions for which solutions in [16] are obtained. Firstly, due to the nature of the fatigue crack herein analysed, the crack assessed was not straight. Secondly, the crack tip front was not precisely perpendicular to the surface analysed, as the different crack lengths measured on either side of the specimen show.

CONCLUSIONS

The combination of the image correlation method and the Muskhelishvili's complex function analysis has proven to be a fast and robust technique for mixed-mode SIF determination. The technique has been used to evaluate SIFs for a crack emanating from a hole in a plate geometry. The crack tip position was also calculated from the displacement fields by means of an edge finding routine.

ACKNOWLEDGEMENTS

The authors would like to acknowledge financial support from the Engineering and Physical Sciences Research Council (EPSRC), UK, grant GR/S18045/01.

REFERENCES

1. Nurse, A.D. and Patterson, E.A. (1998) *Fatigue Fract. Eng. Mater. Struct.* **16**(12):1339–1354.
2. Barker, D. B., Sanford, R. J. and Chona, R. (1985) *Exp. Mech.*, **25**(4):399-405.
3. Díaz, F.A., Yates, J.R. and Patterson, E. A. (2004) *Int. J. Fatigue*, **26**(4):365–376.
4. Yoneyama, S., Morimoto, Y. and Takashi, M. (2004). In *Proceedings of the 12th International Conference on Experimental Mechanics, Bari, Italy*.
5. Hild, F., Roux. S. (2006) *C. R. Mecanique*, **334**.
6. Clocksin, W.F., Quinta da Fonseca, J., Withers, P.J. and Torr, P.H.S. (2002) In *Proceedings of SPIE*, **4790**: 384–395.
7. Sutton, M.A., McNeill, S.R., Helm, J.D. and Chao, Y.J. (1999) *Topics in Applied Physics*, **77**:323–372.
8. Burguete, R. and Patterson, E. A. (2002) In *VAMAS Bulletin* **25**:49–51
9. Da Fonseca, J.Q., Mummery, P.M. and Withers, P. J. (2005) *Journal of Microscopy*, **218**(1):9–21.
10. LaVision GmbH. (1999) *PIV Software Manual: DaVis*. Gottingen, Germany,. www.lavision.de.
11. Muskhelishvili, N. I. (1977) In: *Some Basic Problems of the Mathematical Theory of Elasticity*. Noordhoff International, Leyden, The Netherlands, 4th edition.
12. Sih, G.C., Paris, P.C. and Erdogan, F. (1962) *J. Appl. Mech.* **29**:306–312.
13. Sanford, R.J. and Dally, J.W. (1979) *Eng. Fract. Mech.* **11**(4):621–633.
14. Sonka, M., Hlavac, V. and Boyle, R. (1993) In: *Image Processing, Analysis and Machine Vision*. Chapman & Hall International, London.
15. Press, W.H., Flannery, B.P., Teukolsky, S.A. and Vetterling, W. T. (1986) In: *Numerical recipes: the art of scientific computing, FORTRAN version*. Cambridge: Cambridge University Press.
16. Murakami, Y. editor. (1987) In: *Stress Intensity Factors Handbook*. Pergamon Press, UK.